

RESEARCH PAPER

Synthesis of CuFeS₂ Nanoparticles by One-pot Facile Method

Yaser Vahidshad ^{1*}, Seyed Mohammad Mirkazemi ¹, Muhammad Nawaz Tahir ², Reza Ghasemzadeh ¹ and Wolfgang Tremel ²

¹ School of Metallurgy and Material Engineering, Iran University of Science and Technology, Tehran, Iran

² Institute of Inorganic Chemistry and Analytical Chemistry, Johannes Gutenberg University Mainz, Duesbergweg, Mainz, Germany

ARTICLE INFO

Article History:

Received 02 August 2017

Accepted 24 September 2017

Published 01 October 2017

Keywords:

Chalcopyrite

Heating up Solution Synthesis

Infrared Absorption

Wurtzite

ABSTRACT

Monodisperse copper-iron-sulfide (CuFeS₂) nanoparticles as the infrared light absorbing material (chalcopyrite, 0.65 eV), were synthesized based on facile, one step heating up method, by dissolving of CuCl, FeCl₃ and SC(NH₂)₂ as precursors in oleylamine (OLA) alone or in combination with oleic acid (OA) and 1-octadecene (ODE) as solvent. The phase, size, morphology, and size distribution were controlled by the reaction conditions and temperature. The CuFeS₂ nanoparticles were characterized by transmission electron microscopy, X-ray diffraction, X-ray photoelectron spectroscopy, Raman spectrum and ultraviolet-visible-near infrared. The three main absorbance region was observed in the ultraviolet, visible and infrared as a hybridization of Fe 3d-S 3p among the valence band (Cu 3d-S 3p) and conduction band (Cu 4s-Fe 4s). Well controlled CuFeS₂ triangular pyramidal along with semi-hexagonal and hexagonal shape (~ 20-25 nm) was obtained by using OLA or a mixture of OLA along with OA and ODE, respectively, with 210 °C heating up and 4 h annealing time.

How to cite this article

Vahidshad Y, Mirkazemi S. M, Tahir M. N, Ghasemzadeh R, Tremel W. Synthesis of CuFeS₂ Nanoparticles by One-pot Facile Method. J Nanostruct, 2017; 7(4):284-291.

INTRODUCTION

The structural, optical and electrical properties of I-III-VI₂ compounds can easily be modified in large extent by varying of stoichiometry and chemical composition. The high absorption coefficient, a changeable electrical conductivity from p-type to n-type with change of intrinsic composition ratio besides tuning of band gap (0.6 eV for CuFeS₂ to 3.5 eV for CuAlS₂) [1-6] can be employed in the multi-junction solar cells [7, 8], lithium ion battery [9], thermoelectrics [10] and photocatalysts [11]. General creation method to produce CuFeS₂ compounds become increasingly important with respect to their unique physical and chemical properties for potential applications.

* Corresponding Author Email: yvahidshad@yahoo.com

Wet chemistry process such as thermolysis [12], hot injection [13], solvothermal [14] hydrothermal [15] and high temperature solid solution [16] and Bridgman technique [17] do not require post annealing treatments and are usually crystalline [18,19].

One-pot thermolysis method as one of the simple wet synthesis methods to achieve mentioned properties can be used to produce of CuFeS₂ colloidal that applicable as Ink to produce of vacuum free thin films. In this research, we considered the effect of solvents and temperature on the structural and optical properties of CuFeS₂ compound that synthesis by thermolysis technique.



This work is licensed under the Creative Commons Attribution 4.0 International License.

To view a copy of this license, visit <http://creativecommons.org/licenses/by/4.0/>.

MATERIALS AND METHODS

CuFeS₂ nanoparticles were synthesized by mixing copper chloride (CuCl, Sigma-Aldrich), iron trichloride (FeCl₃, Sigma-Aldrich), and thiourea (CH₄N₂S, Fisher) as precursors and oleylamine (OLA) (C₁₈H₃₇N, Acros), oleic acid (OA) (C₁₈H₃₄O₂, Fisher), and 1-octadecene (ODE) (C₁₈H₃₆, Acros) as coordinating solvent, capping agent, and noncoordinating solvent under Ar. In a typical synthesis, 0.5 mmol of CuCl, 0.5 mmol of FeCl₃, and 2 mmol of thiourea (TU) were dissolved in OLA, OA, and ODE under Ar at room temperature using the Schlenk technique. The contents of the flask were evacuated at 90 °C for 45 min. After that, the flask atmosphere was changed to argon, and the reaction mixture was heated to 210 °C with a rate of 18–20 °C/min. During the heating process, smoke began to evolve at a temperature about 140 °C, and the color turned darker, indicating nucleation and growth phenomena. The flask was held at the above-mentioned temperature for 4 h before cooling it to room temperature (Fig. 1). Then, 30 mL of ethanol was added to the reaction flask and centrifuged for 10 min (9000 rpm) to collect the product. For XRD and XPS analysis, the process of washing was repeated several times and finally dried at 80 °C for 5 h in air condition. The structure, morphology, and optical properties of the products were characterized by X-ray diffraction analysis (Mo K α radiation, energy-dispersive detector SOLX), Raman spectrum was recorded by FT-Raman NXR FT-Raman module, Thermo Nicolet that thermoelectrically cooled InGaAs Detector (~0.9–2 μ m) with CaF₂ Beamsplitter Nitrogen-cooled NXR Genie Germanium Detector (~0.9–1.6 μ m), X-ray photoelectron spectroscopy (high-resolution excitation in the laboratory UV light and vacuum: 10–10 Pa), EDX-INCA350 Energy (FE-SEM/Quanta 200 FEG, 30 kV), the transmission electron microscope (Philips EM420 microscope operating at an acceleration voltage of 120 kV), FT-IR spectroscopy (acquired on a Mattson

Instruments 2030 Galaxy spectrometer), UV–Vis–NIR absorbance spectroscopy (Ocean Optics Ins. USB-4000), and photoluminescence spectroscopy (Bruins Omega-10 spectrometer).

RESULTS AND DISCUSSION

Fig. 1 shows the X-ray powder diffraction of CuFeS₂ nanoparticles synthesized with various temperatures at 1 hr (samples A, B and D) and 4 hr (samples F, G and H). A close observation of the X-ray diffraction peaks of the samples shows the wurtzite structure excite (wurtzite simulated [12]) along with chalcopyrite structure (JCPDS 01-083-0984) depending on the reaction temperature (polytypism). However, it is worth to mention that there is no binary sulfide, along with main ternary phases of CuFeS₂. Fig. 1 reveals thermodynamically chalcopyrite structure is more stable in higher temperature. In fact, the wurtzite structure reform to chalcopyrite structure in higher temperature. Additionally, by increasing temperature more than 270 °C (310 °C for sample H) the CuFeS₂ compound decomposed to Cu_{2-x}S. It is observed the chalcopyrite structure has been stabilized by increasing of OA. As seen in Fig. 1 (samples F, I and J), by using OA beside OLA along with ODE, the chalcopyrite structure can be produced as a major structure. The ODE as noncoordinating solvent was used to improve the morphology with more satiric effect. Other than oleic acid, the reaction temperature is also an important parameter to the formation of chalcopyrite structure (Fig. 1). However, reaction time and heating rate did not any influence on crystal structure (samples C, D, E and F).

Frequency Raman spectroscopy to identify the molecular structure is very suitable for the determination of molecular vibrations, rotating and evaluate the geometry and symmetry of the molecule is even possible. In some cases where there is no possibility to determine the molecular structure, the frequency can be recorded on the

Table 1. Experimental detail for one-pot thermolysis synthesis of CuFeS₂.

Sample No.	Solvents	Heating rate	Reaction temperature	Synthesis duration	Crystalline structure
A-CFS-WOA-M3	20cc OLA	18-20 °C/min	150 °C	1 hr	Wurtzite
B-CFS-WOA-M4	20cc OLA	18-20 °C/min	180 °C	1 hr	Less Chalcopyrite + More Wurtzite
C-CFS-WOA-M6	20cc OLA	8-9 °C/min	210 °C	1 hr	Chalcopyrite + Wurtzite
D-CFS-WOA-M7	20cc OLA	18-20 °C/min	210 °C	1 hr	Chalcopyrite + Wurtzite
E-CFS-WOA-M8	20cc OLA	8-9 °C/min	210 °C	4 hr	Chalcopyrite + Wurtzite
F-CFS-WOA-M9	20cc OLA	18-20 °C/min	210 °C	4 hr	Chalcopyrite + Wurtzite
G-CFS-WOA-M10	20cc OLA	18-20 °C/min	260 °C	4 hr	Chalcopyrite
H-CFS-WOA-M11	20cc OLA	18-20 °C/min	310 °C	4 hr	Decomposed to Cu _{2-x} S
I-CFS-WOA-M12	20ccOLA+4ccOA+6ccODE	18-20 °C/min	210 °C	4 hr	More Chalcopyrite + Less Wurtzite
J-CFS-WOA-M13	20ccOLA+2ccOA+3ccODE	18-20 °C/min	210 °C	4 hr	More Chalcopyrite + Less Wurtzite

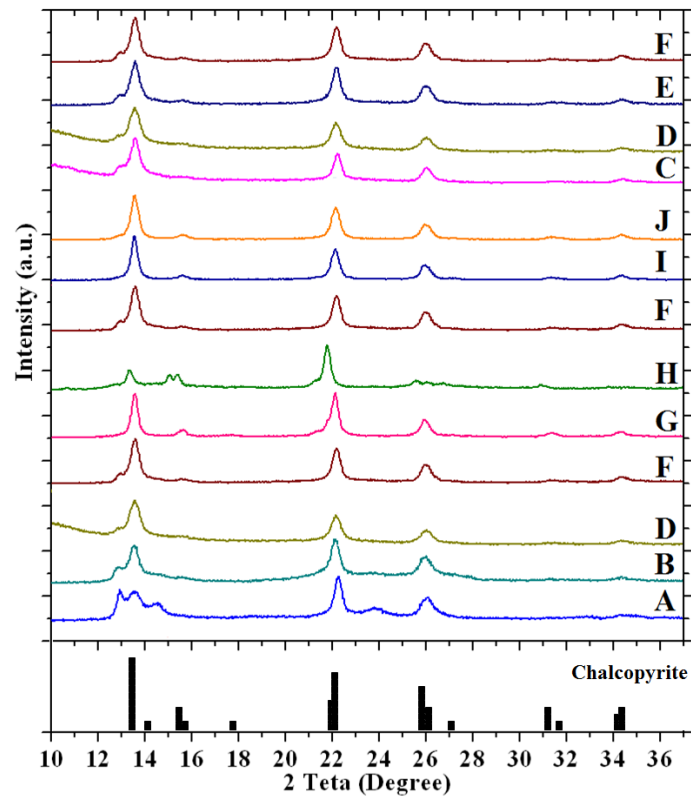


Fig. 1. PXRD patterns of the synthesized CuFeS₂ at various synthesized conditions that mentions in Table 1.

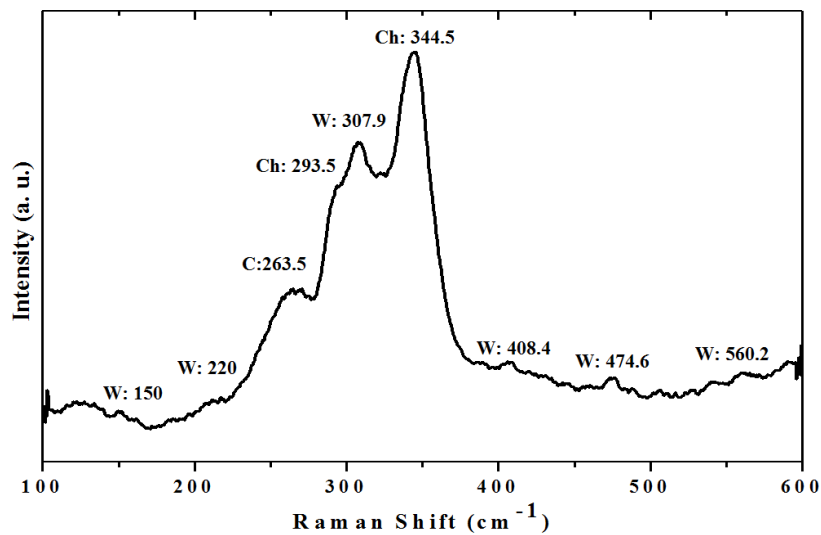


Fig. 2. Raman spectrum of CFS-9 (sample 9) synthesized by thermolysis method.

basis of the atom, in a molecule can be studied. Since the number of Raman active modes is different for each phase, this technique allows one to unambiguously detect the different phase,

which did not have any special Raman peaks in literature; many references were taken in order to distinguish Raman peaks in our samples [12. 20-23]. Spectrums showed the characteristic

bands of the wurtzite (marked W), chalcopyrite (marked Ch) and covellite (marked C) phases (Fig. 2). These results were confirmed in the results of XRD analysis. The optical mode peaks located at 150, 220, 307.9, 408.4, 474.6 and 560.2 cm⁻¹ can be attributed to wurtzite phase, the optical mode peaks located 293.5, 344.5 cm⁻¹ can be attributed to chalcopyrite and the peak of 263.5 cm⁻¹ can be attributed to covellite.

Formation of chalcopyrite or wurtzite CuInS₂ or structure can be attributed to initially formed nuclei of Cu_{2-x}S structure [24]. When the first seed formed as Cu₂S (Chalcite, hexagonal structure) after cation exchange reaction, the CuInS₂ formed as wurtzite structure and if the first nuclei formed as Cu₉S₅ (Digenite, FCC anti-fluorite structure) after cation exchange reaction the CuInS₂ formed as chalcopyrite [24-28]. Kuzuya [27] and Koo [29] showed that the OLA can stabilize the wurtzite structure in CuInS₂.

Usually, the shapes of nanocrystals are controlled first by the nucleation stage and then by the particles growth stage. These parameters depend on solvent, capping agent and temperature [30-32].

Fig. 3 shows effect of reaction temperature on the morphology. In our system, it is found

that when the crystalline structure is wurtzite (low temperature synthesis) for sample A and B, the shape of nanoparticles is grown along <001> direction as a result elongated nanocrystal obtained. When the chalcopyrite structure produced (by increasing synthesis temperature) for sample D, the polyhedron nanocrystals can be seen along with elongated nanocrystals (Fig. 3). In fact, in the special condition (border condition, reaction temperature more than 180 °C), the reaction proceeds and the chalcopyrite structure could be grown on the initial wurtzite crystal by stacking fault mechanism as a result the shape was similar to the semi-hexagonal shape.

The effect of oleic acid and oleylamine solvent ratio on the morphology of nanocrystals can be observed in the Fig. 4. The hexagonal shape of CuFeS₂ nanocrystals can be attributed to wurtzite structure and the trigonal shape of CuFeS₂ nanocrystals can be attributed to chalcopyrite structure. Same as previous, the chalcopyrite structure could be grown on the initial wurtzite crystal (border condition, a mixture of OLA and OA solvents) as a result the shape was similar to the semi-hexagonal shape. Fig. 4 shows a TEM micrograph of the nanoparticles synthesized with different OA to OLA molar ratio at 210 °C for 4 h.

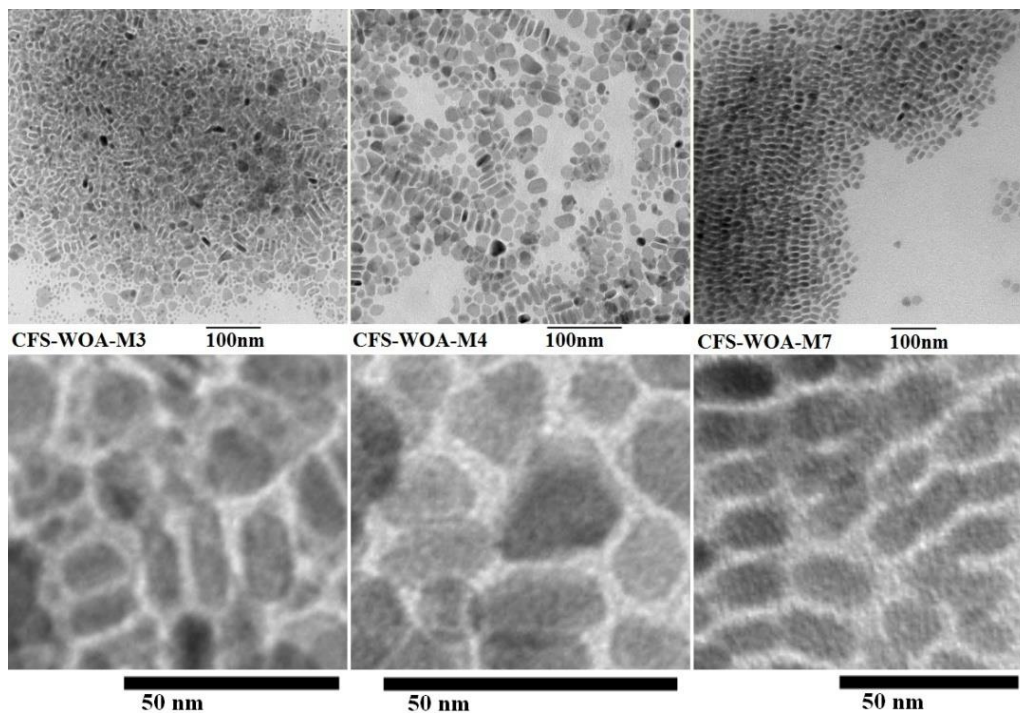


Fig. 3. Effect of different temperatures on the morphology of synthesized nanocrystals.

When the ratio of oleic acid increased compared to oleylamine, 0 ml OA for sample F < 4 ml OA for the sample I < 6 ml for sample J, mixture of the semi-hexagonal (chalcopyrite-wurtzite polytypism) and hexagonal (wurtzite) shape (sample F) changed to semi-hexagonal and triangular (chalcopyrite) shape (samples I and J).

To study the composition and chemical state of the compounds, the samples of CuFeS₂ were examined by X-ray photoelectron spectroscopy (XPS). The binding energies in the XPS analysis are corrected for specimen charging by referencing the C 1s and O 1s to binding energy of 285.0 eV and 532.2 eV, respectively. For the CFS-WOA-M9 and CFS-WOA-M12 samples, all the Cu-related, Fe-related and S-related peaks appeared in the XPS spectrum (Fig. 5). The Cu 2p³ and Cu 2p¹ peaks are located in 931.4 eV and 951.4 eV for both of them that are shown Fig. 5. They confirm that the valence states of Cu ions are +1 in all synthesized samples, due to the absence of the satellite peak at about 944.0 eV for Cu²⁺. Moreover, the electron binding energy of Fe 2p³ and Fe 2p¹ position at 712.2 and 726.6 eV and 711.4 and 725.0 eV for CFS-WOA-M9 and CFS-WOA-M12, respectively, confirm that the valence state of Fe in the structure is 3+ for solid solution samples. The electron binding energy of

S 2p³ that are observed at 163.4 for samples is attributed to S²⁻ [13, 33-36].

The electronic structure for CuFeS₂ (Fig. 6) reveals that iron d-orbitals are hybridized with p-orbital of sulfur atoms which lead to formed intermediate band (including Fe 3d and S 3p) are located between occupied valence band composed of Cu 3d and S 3p orbital and unoccupied conduction band, including of Cu 4s and Fe 4s states [35-39].

The optical properties of CuFeS₂ compound dispersed in n-hexan-are measured at room temperature with UV-Vis-NIR absorption (Fig. 7). The derived data shows that the edge of the absorption spectrum is around three main ultraviolet, visible and near infrared regions. The first edge absorbance around the 630 nm attributed to transition electron from valence band that was formed based on the hybridization of the Cu 3d orbitals and the S 3p orbitals to conduction band that was formed based on the hybridization of the Cu 4s orbitals and the Fe 4s orbitals for samples F-CFS-WOA-9, I-CFS-WOA-10 and J-CFS-WOA-12.

A strong absorption region is observed on the lower energy around the 1127 nm that attributed to inter-band that was formed based on the

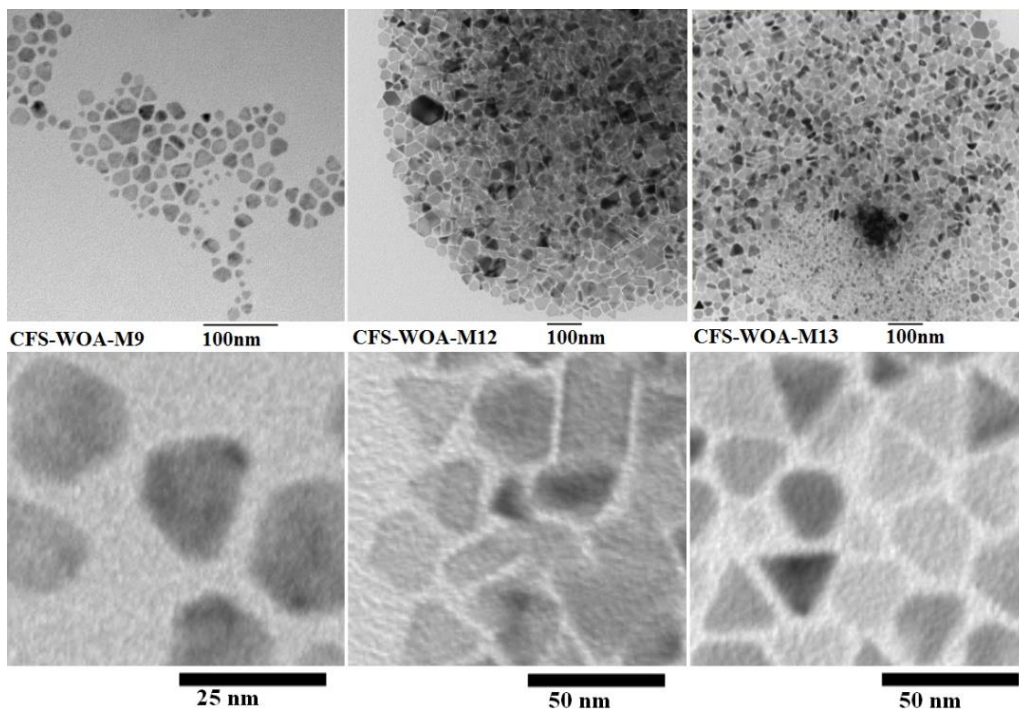


Fig. 4. Effect of different solvents on the morphology of synthesized nanoparticles.

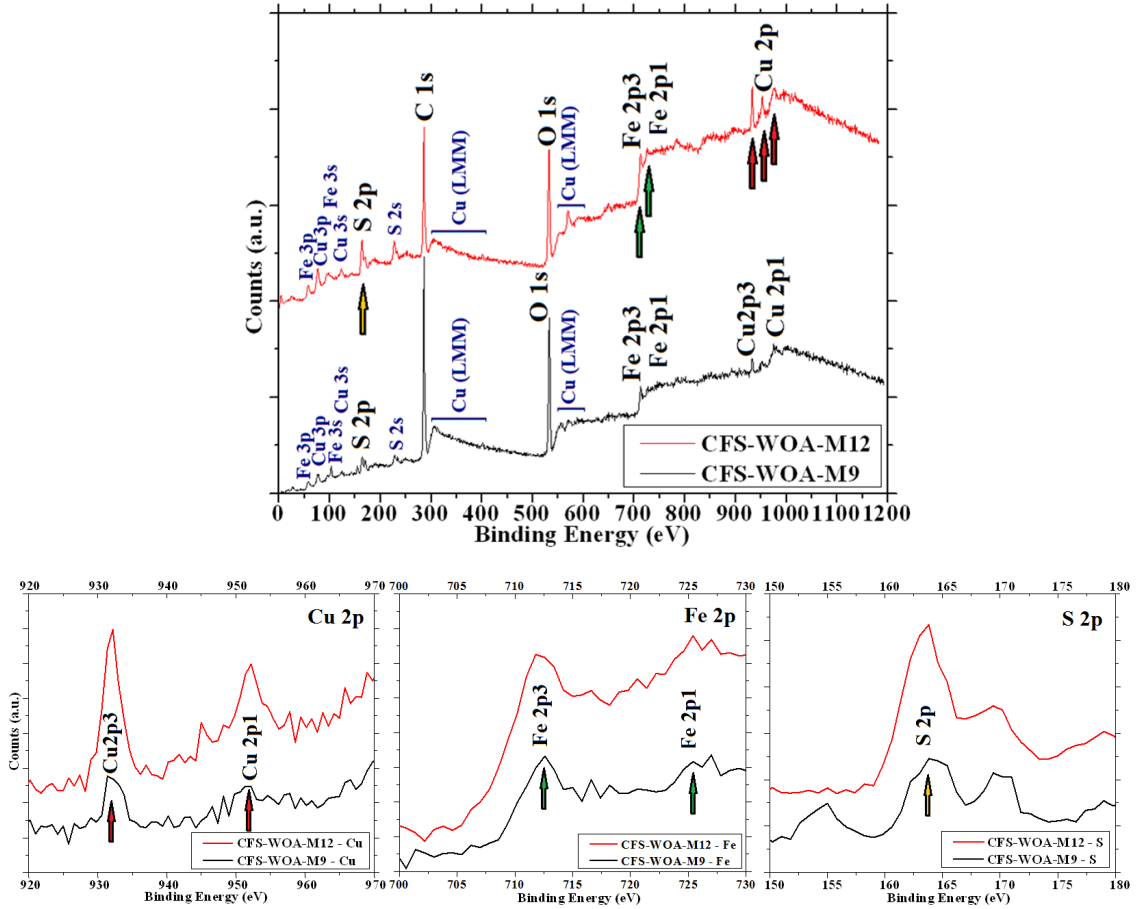


Fig. 5. Whole XPS spectra and high resolution XPS spectra of Cu 2p, Fe 2p, S 2p to of CFS-WOA-M9 (black) and CFS-WOA-M12 (red) compounds.

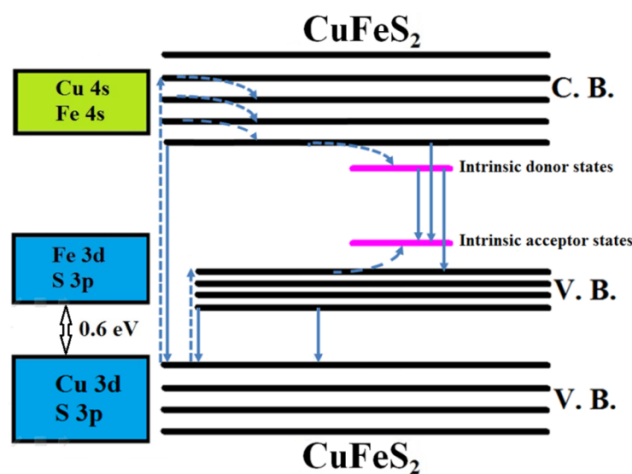


Fig. 6. Schematic of the possible optical absorption spectra and relaxation pathways of synthesized CuFeS₂ nanoparticles.

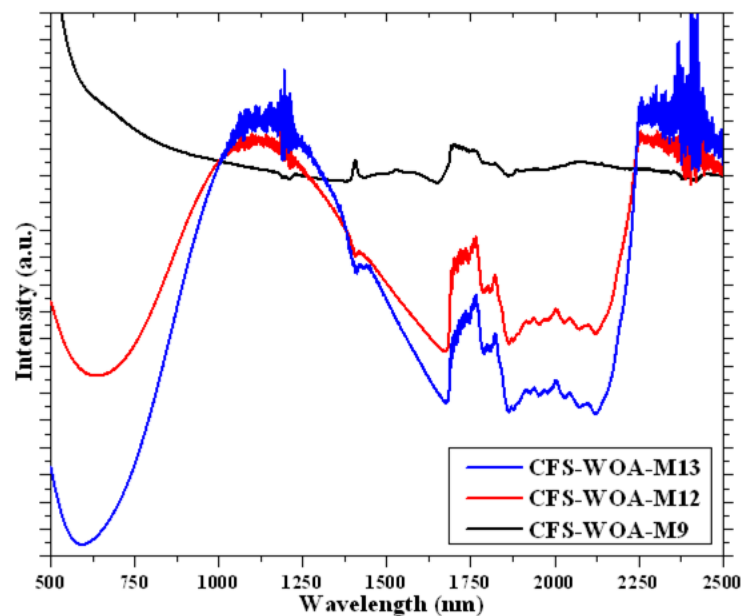


Fig. 7. Optical absorbance spectrum of synthesized CuFeS₂ nanoparticles.

hybridization of the Fe 3d orbitals and the S 3p orbitals to conduction band that was formed based on the hybridization of the Cu 4s orbitals and the Fe 4s orbitals. The d-d absorption based transition from the Cu 3d-S 3p orbitals hybridization to the Fe 3d-S 3p orbitals hybridization that observed around the 2060 nm. Other absorption regions between 1500-1850 nm and 2250-2500 nm can be attributed to charge transfer that based on the transition from Cu 3d or Fe 3d orbitals to ligand orbitals or vice versa (Fig. 7).

CONCLUSION

A simple and convenient one-pot synthesis method was developed for the controlled synthesis of chalcopyrite and wurtzite structure by controlling synthesis temperature and solvent. The structure of CuFeS₂ could be changed from wurtzite to chalcopyrite by controlling the synthesis temperature from 150 °C to 270 °C and using OLA alone to a mixture of OLA and OA. Because the wurtzite structure produced in the first stage, the further growth crystal with the chalcopyrite structure result that both of chalcopyrite-wurtzite crystalline structure existing in every nanocrystals (polytypism). The shape of nanoparticles could be changed from hexagonal to trigonal based on free surface energy by changing the functional groups of solvents, reaction temperature or time.

ACKNOWLEDGMENT

This research was defined and supported by from the Iran university of Science and Technology. This research was supported by Professor Wolfgang Tremel at Johannes Gutenberg-University of Mainz.

CONFLICT OF INTEREST

The authors declare that there are no conflicts of interest regarding the publication of this manuscript.

REFERENCES

1. Y. Mikhлина, Y. Tomashevicha, V. Tausonb, D. Vyalikhc, S. Molodtsovc, R. Szargan, A comparative X-ray absorption near-edge structure study of bornite, Cu₅FeS₄, and chalcopyrite, CuFeS₂. *J. Electron. Spectrosc. Relat. Phenom.* 2005; 142 (1), 83-88.
2. Y. Vahidshad, M. N. Tahir, A. Iiraji-Zad, S. M. Mirkazemi, R. Ghazemzadeh, Hannah Huesmann, W. Tremel, Structural and optical study of Ga³⁺ substitution in CuInS₂ nanoparticles synthesized by a one-pot facile method. *J. Phys. Chem. C.* 2014; 118 (42), 24670-24679.
3. J. Hu, Qi. Lu, B. Deng, K. Tang, Y. Qian, Y. Li, G. Zhou, X. Liu, A hydrothermal reaction to synthesize CuFeS₂ nanorods. *Inorg. Chem. Commun.* 1999; 2 (12), 569-571.
4. Y. Vahidshad, M. N. Tahir, A. Iiraji-Zad, S. M. Mirkazemi, R. Ghazemzadeh, W. Tremel, Structural and Optical Properties of Fe and Zn Substitution in CuInS₂ Nanoparticles Synthesized by a One-Pot Facile Method. *J. Mater. Chem. C.* 2015; 3 (4), 889-898.
5. E. J. Silvester, T. W. Healy, F. Grieser, B. A. Sexton, Hydrothermal preparation and characterization of optically

- transparent colloidal chalcocopyrite (CuFeS₂). *Langmuir*. 1991; 7 (1), 19-22.
- Y. Vahidshad, A. Iraj-Zad, R. Ghasemzadeh, S. M. Mirkazemi, A. Masoud, Structural and optical characterization of nanocrystalline CuAlS₂ chalcocopyrite synthesized by polyol method in autoclave. *Int. J. Mod. Phys. B*. 2012; 26 (31), 1250179 (1-12).
 - D. L. Young, J. Abushama, R. Noufi, X. Li, J. Keane, T. A. Gessert, J. S. Ward, M. Contreras, M. Symko-Davies, T. J. Coutts, Photovoltaic Specialists Conference. A new thin-film CuGaSe₂/Cu(In,Ga)Se₂ bifacial, tandem solar cell with both junctions formed simultaneously. 29th IEEE PV Specialists Conference-New Orleans, Louisiana May 20-24. 2002; 608-611.
 - J. Song, S. S. Li, C. H. Huang, T. J. Anderson, O. D. Crisalle, Modeling and simulation of a CuGaSe₂/Cu(In_{1-x}Ga_x)Se₂ tandem solar cell. 3rd World Conference on Photovoltaic Energy Conversion. Osaka, 1, May 18-18. 2003; 555-558.
 - W. Ding, X. Wang, H. Peng, L. Hu, Electrochemical performance of the chalcocopyrite CuFeS₂ as cathode for lithium ion battery. *Mater. Chem. Phys.* 2013; 137 (3), 872-876.
 - N. Tsujii, T. Mori, Y. Isoda, Phase stability and thermoelectric properties of CuFeS₂-based magnetic semiconductor. *J. Electron. Mater.* 2014; 43 (6), 2371-2375.
 - S. Kang, B. S. Kwak, M. Park, K. M. Jeong, S.-M. Park, M. Kang, Synthesis of Core@shell structured CuFeS₂@TiO₂ magnetic nanomaterial and its application for hydrogen production by methanol aqueous solution photosplitting. *Bull. Korean Chem. Soc.* 2014; 35 (9), 2813-2817.
 - P. Kumar, S. Uma, R. Nagarajan, Precursor driven one pot synthesis of wurtzite and chalcocopyrite CuFeS₂. *Chem. Commun.* 2013; 49 (66), 7316-7318.
 - Y.-H. A. Wang, N. Bao, A. Gupta, Shape-controlled synthesis of semiconducting CuFeS₂ nanocrystals. *Solid State Sci.* 2010; 12 (3), 387-390.
 - Animesh Layek, Arka Dey, Joydeep Datta, Mrinmay Das, Partha pratim ray, Novel CuFeS₂ pellet behaves like a portable signal transporting network: studies of immittance. *RSC Adv.* 2015; 5 (44), 34682-34689.
 - K.-T. Chen, C.-J. Chiang, D. Ray, Hydrothermal synthesis of chalcocopyrite using an environmental friendly chelating agent. *Mater. Lett.* 2013; 98, 270-272.
 - S. D. Disale, S. S. Garje, A Convenient synthesis of nanocrystalline chalcocopyrite, CuFeS₂ using single-source precursors. *Appl. Organometal. Chem.* 2009; 23 (12), 492-497.
 - K. Sato, Y. Harada, M. Taguchi, S. Shin, A. Fujimori, Characterization of Fe 3d States in CuFeS₂ by Resonant X-ray Emission Spectroscopy. *Phys. Status Solidi A*. 2009; 206 (5), 1096-1100.
 - L. Shi, C. Pei, Q. Li, Ordered arrays of shape tunable CuInS₂ nanostructures, from nanotubes to Nano test tubes and nanowires. *Nanoscale*. 2010; 2 (10), 2126-2130.
 - D. Pan, L. An, Z. Sun, W. Hou, Y. Yang, Z. Yang, Y. Lu, Synthesis of Cu-In-S ternary nanocrystals with tunable structure and composition. *J. Am. Chem. Soc.* 2008; 130 (17), 5620-5621.
 - B. Li, L. Huang, M. Zhong, Z. Wei, J. Li, Electrical and magnetic properties of FeS₂ and CuFeS₂ nanoplates. *RSC Advances*. 2015; 5 (11), 91103-91107.
 - T. P. Mernagh, A. G. Trudu, A laser Raman microprobe study of some geologically important sulphide minerals. *Chem. Geol.* 1993; 103 (1-4), 113-127.
 - J. Łażewski, H. Neumann, K. Parlinski, Ab initio characterization of magnetic CuFeS₂. *Phys. Rev. B*. 2004; 70 (19), 195206 (1-7).
 - K. Aup-Ngoen, T. Thongtem, S. Thongtem, A. Phuruangrat, Cyclic microwave-assisted synthesis of CuFeS₂ nanoparticles using biomolecules as sources of sulfur and complexing agent. *Mater. Lett.* 2013; 101, 9-12.
 - M. H. Valdés, M. Berruet, A. Goossens, M. Vázquez, Spray deposition of CuInS₂ on electrodeposited ZnO for low-cost solar cells. *Surf. Coat. Tech.* 2010; 204 (24), 3995-4000.
 - G. Will, E. Hinze, A. Rahman, M. Abdelrahman, Crystal structure analysis and refinement of Digenite, Cu₁₈S₈, in the temperature range 20 to 500°C under controlled sulfur partial pressure. *Eur. J. Mineral.* 2002; 14 (3), 591-598.
 - S. T. Connor, C. M. Hsu, B. D. Weil, S. Aloni, Y. Cui, Phase Transformation of biphasic Cu₂S-CuInS₂ to monophasic CuInS₂ nanorods. *J. Am. Chem. Soc.* 2009; 131 (13), 4962-4966.
 - T. Kuzuya, Y. Hamanaka, K. Itoh, T. Kino, K. Sumiyama, Y. Fukunaka, S. Hirai, Phase control and its mechanism of CuInS₂ nanoparticles. *J. Colloid Interface Sci.* 2012; 388 (1), 137-143.
 - M. B. Sigman, Jr., A. Ghezlbash, T. Hanrath, A. E. Saunders, F. Lee, B. A. Korgel, Solventless synthesis of monodisperse Cu₂S nanorods, nanodisks. *J. Am. Chem. Soc.* 2003; 125 (51), 16050-16057.
 - B. Koo, R. N. Patel, B. A. Korgel, Wurtzite-chalcocopyrite polytypism in CuInS₂ nanodisks. *Chem. Mater.* 2009; 21 (9), 1962-1966.
 - J.-J. Wang, J.-S. Hu, Y.-G. Guo, L.-J. Wan, Wurtzite Cu₂ZnSnSe₄ nanocrystals for high-performance organic-inorganic hybrid photodetectors. *NPG Asia Mater.* 2012; 4 (8), 1-10.
 - S. Kumar, T. Nann, Shape control of II-VI semiconductor nanomaterials. *Small*. 2006; 2 (3), 316-329.
 - E. Witt, J. Kolny-Olesiak, Recent Developments in Colloidal Synthesis of CuInSe₂ Nanoparticles. *Chem. Eur. J.* 2013; 19 (30), 9746-9753.
 - D. J. Vaughan, K. E. R. England, G. H. Kelsall, Q. Yin, Electrochemical oxidation of chalcocopyrite (CuFeS₂) and the related metal-enriched derivatives Cu₄Fe₅S₉, Cu₉Fe₃S₁₆, and Cu₉Fe₈S₁₆. *Am. Mineral.* 1995; 80 (7-8), 725-731.
 - M. X. Wang, L. S. Wang, G. H. Yue, X. Wang, P. X. Yan, D. L. Peng, Single crystal of CuFeS₂ nanowires synthesized through solventothermal process. *Mater. Chem. Phys.* 2009; 115 (1), 147-150.
 - D. F. Marrón, A. Martí and A. Luque, Thin-film intermediate band chalcocopyrite solar cells. *Thin Solid Films*. 2009; 517 (7), 2452-2454.
 - Y. Mikhlin, Y. Tomashevich, V. Tauson, D. Vyalikh, S. Molodtsov, R. Szargan, A comparative X-ray absorption near-edge structure study of bornite, Cu₅FeS₄, and chalcocopyrite, CuFeS₂. *J. Electron Spectrosc. Relat. Phenom.* 2005; 142 (1), 83-88.
 - T. Kambara, Optical properties of a magnetic semiconductor: chalcocopyrite CuFeS. II. calculated Electronic structures of CuGaS₂:Fe and CuFeS₂. *J. Phys. Soc. Jpn.* 1974; 36 (6), 1625-1635.
 - J. A. Tossell, D. S. Urch, D. J. Vaughan and G. Wiech, The Electronic structure of CuFeS₂, chalcocopyrite, from X-ray emission and X-ray photoelectron spectroscopy and Xα calculations. *J. Chem. Phys.* 1982; 77 (1), 77-82.
 - C. Tablero and D. F. Marron, Analysis of the electronic structure of modified CuGaS₂ with selected substitutional impurities: prospects for intermediate-band thin film solar cells based on Cu-containing chalcocopyrites. *J. Phys. Chem. C*. 2010; 114 (6), 2756-2763.